Biocompatibility of Biomaterials

Hemant Kumar Raut,[1Φ] Rupambika Das,[1Φ] Liu Ziqian,[3] Liu Xiaoling,[3*] Seeram Ramakrishna[2*]

[1] *Division of Engineering Product Development, Singapore University of Technology and Design, 8 Somapah Rd, Singapore 487372, Republic of Singapore*

[2] *Centre for Nanofibers & Nanotechnology, Department of Mechanical Engineering, National University of Singapore, Singapore 117574, Singapore*

[3] *Department of Mechanical, Materials and Manufacturing Engineering, The University of Nottingham Ningbo China, 199 Taikang East Road Ningbo, 315100, China*

There is a vast number of biomaterials ranging from drug-eluting stents, coated implants, drug delivery devices and artificial organs, among others, that have been developed in recent years. However, translation of many of these biomaterials to clinic is often plagued by biocompatibility challenges. This review focuses on strategies implemented in some of the recently developed biomaterials – particularly for soft and hard tissue regeneration, organ manufacturing and disease remediation – to overcome potential foreign body response to the incorporation of the biomaterials in the host.

A range of materials are used or synthesized today to serve as biomaterials [illustrated in Figure 1 along with a comprehensive list given in Table 1A-D]. For instance, metal-based biomaterials (such as stainless steels, Ti and Co-based alloys) are used for load bearing application. They range from simple wires and screws to fracture fixation plates and total joint prostheses (artificial joints) for hips, knees, shoulders and ankles[1]. Similarly, ceramics are used in dentistry applications (in crowns, cements and dentures)[2]. Polymers (natural polymers like fibrin, gelatin, collagen as well as synthetic polymers like PEG, PLGA, PMMA *etc.*) too find applications in a wide variety of biomaterials ranging from facial prostheses to tracheal tubes, contact lenses and medical adhesives and sealants[2]. Composites (fibre-reinforced and CNT-polymer composites) owing to their light-weight and high strength characteristics, also have made inroads into the biomedical field (prosthetic limbs)[3,4]. Additionally, a vast number of natural materials (materials derived from animals or plants) have been incorporated in biomaterials[5]. These natural materials with characteristics similar to that of human body, have been found to carry specific protein binding sites and other biochemical signals that promote

* Corresponding authors' email addresses: seeram@nus.edu.sg; Φ The authors have contributed equally.

tissue healing and integration. The natural materials integrate with the cells due to cell-ECM integration and leads to cell migration, proliferation and differentiation[6].

However, the success of biomaterials depends inevitably on their acceptability by the human body. It is essential that a biomaterial (a) does not elicit any undesirable effects such as cytotoxicity, genotoxicity, mutagenicity, carcinogenicity and immunogenicity in the recipient or beneficiary, (b) perform its desired function with respect to a medical therapy and (c) generate the most appropriate beneficial cellular or tissue response[7,8]. To evaluate the biocompatibility, biomaterials are mandatorily subjected to a number of different tests which are performed as recommended by various regulatory organizations. These tests consist of a sequence of research protocols as described and regulated in many countries, for determining the safety of the biomaterials for clinical application in humans[7]. Lack of biocompatibility remains a key concern for biomaterials[9]. For example, premature wear and dislocation of hip and knee prostheses, infection and rejection of dental implants, restenosis and blockage in coronary stents *etc*[10,11]. Additionally, it has been estimated that 80% of the infections in hospitals are due to bacterial biofilms formation on surfaces of biomaterials, implants or surgical devices. These biofilms have up to 1000 times higher resistance to antimicrobial chemicals than bacteria in the planktonic form[12,13]. Hence it is crucial that the biomaterials pass rigorous biocompatibility evaluations. In recent times, the term "biocompatibility" has been redefined as - "the ability of a material to perform its desired functions with respect to a medical therapy, to induce an appropriate host response in a specific application and to interact with living systems without having any risk of injury, toxicity, or rejection by the immune system and undesirable or inappropriate local or systemic effects"[11].

This comprehensive review consolidates the findings from some of the most important recent works on biomaterials, particularly in the area of biomaterials for soft and hard tissue regeneration, arterial blockage remediation, organ manufacturing, and focuses on strategies addressing the biocompatibility of these biomaterials.

Biocompatibility Considerations

Biological compatibility: It is essential that biomaterials do not produce any undesirable local or systemic effects from its host. Conversely, they must not be affected by the physiological conditions prevailing at the implant site. To give an example of the latter, saliva and bacteria found in the oral cavity, are corrosive in nature and often corrode dental restorative materials

[14]. Biocompatibility requirements or foreign body response depends on a few factors such as contact duration, morphology, degradation rate, porosity, shape, size and sterility[15]. For example, a cardiovascular implant or device intended for transient diagnostics or therapeutic purposes, must limit its interaction with blood flow[16,17]. On the other hand, a replacement plate of a cranial bone or a hip implant inserted into the femur must maximize its interaction with bone cells to enable rapid bone-tissue integration (osteointegration). It also needs to support cellular activity, including the facilitation of molecular and mechanical signaling, to optimize tissue regeneration[18]. Also, if the device or tissue implantation produces an immune response, it can lead to acute and chronic inflammatory consequences[19]. Consequently, biomaterials are integrated with approaches enabling localized and/or intermittent drug delivery.

Tri-biological factors such as friction, wear and corrosion play an important role in case of implants because of the latter's use in conditions involving loading and friction (e.g., hip, knee and spine prosthesis). For example, metallic implants have a higher propensity for corrosion in biological systems that could lead to release of metallic ions (such as Ni, Co and Cr) from the implants causing allergic reactions[20]. That is why surface treatments of these biomaterials is important to suppress any potential immunogenic response [a detail list of surface engineering approaches is given in Table 3]. For instance, if the surface is made hydrophilic, it interacts with the surrounding tissue to minimize tissue reaction[21]. Many metallic implants (including the most commonly used Ti-based implants) are coated with Ta which exhibits excellent biocompatibility[22]. In many cases, naturally derived polymers such as dextran, alginate, chitosan and hyaluroran, are also used as coatings on implants. In recent times, a variety of multifunctional biocompatible coatings have also been investigated. Chief among these are hydroxyapatite (HA) coatings that promote cell growth, ceramics and diamond like carbon (DLC) coatings that improve wear resistance and ionic implantations that decrease the release of heavy ions into the body[23]. Particularly in case of orthopedic implants, since bone-mineral apatite share chemical similarities with HA, the latter has been extensively applied to orthopedic implants. In fact, in conventional Ti-based implants, hydroxyapatite (HAP) coatings have been widely studied and shown to promote osteointegration [as shown in Fig 2A]. HA coatings deposited onto metallic implants can promote early bonding of bones which aid in biological fixation. HA has also proven to be a biocompatible substitute to the previously used polymethyl methacrylate (PMMA) based "bone cement" used in orthopedic implant that was later found to be responsible for the "cement disease". Basically, PMMA produces unwanted local heat due to an exothermic reaction during its polymerization and the un-polymerized

MMA residue is cytotoxic[24]. Alternative bio-functionalization of metallic implants are performed using Calcium Phosphate (CaP) or Dicalcium phosphate dehydrate (DCPC) coatings that show improved osteointegration [Fig 2B][6,25]. In addition, bio-inert ceramic (such as alumina and zirconia) based biomaterials have been reinforced with HA coatings to impart both wear resistance and bioactive properties to biomaterials for bone remediation[26,27]. Diamond-like carbon (DLC) coatings, because of their low coefficient of friction (0.1) and excellent biocompatibility, have been applied to TiN implants for total join arthroplasty to mitigate the risk of wear and implant loosening[28]. However, de-cohesion of these intrinsically brittle films and possibility of localized corrosion still limit their use in high load implant applications.

Additionally, mechanical testing of these coatings has raised concerns about their adhesion with implants and the former's wear and fatigue properties. These durability factors become particularly important when long-term implant residency and cyclic motion between the implant and human bone are involved[29]. A strategy to circumvent this challenge is to use porous scaffolds along with HA embedded inside. For examples, a recent work demonstrated that micro-porous scaffold [comprising poly (γ-benzyl-L-glutamate)-modified hydroxyapatite/(poly (L-lactic acid) (PBLG-g-HA/PLLA)] show higher levels of bone integration (and regeneration) in comparison to monolithic poly (L-lactic acid) (PLLA) scaffolds [Fig 2A][30]. In fact, use of nano-porous scaffolds comprising fibrous poly-L-lactide (NF-PLLA) have been shown to facilitate vascularization[31]. Incorporation of porosity directly onto state-of-the-art Ti-based implants have been performed through electrochemical anodization of the surface that produces a porous surface layer of titania nanotubes. Onto this porous surface, HAP coating can adhere well [Figure 2(C1-C3] and can promote protein adsorption, osteoblast cell adhesion and spreading [Figure 2(C4)][32]. On the contrary, metallic stents, incorporated for unblocking of constricted arteries, need to be bio-inert to avoid redeposition of arterial plaque leading to thrombosis and hyperplasia[33]. Recently, stents coated PLGA-chitosan nanofibers have shown reduced platelet adhesion [Fig 2(D)][34,35,36].

Biomechanical compatibility: Several biomaterials such as implants, stents, flexible sensors and diagnostic devices must function in biomechanical environments. When designing such biomaterials, it is essential to consider the physiological loading conditions (axial rotation, flexion extension and lateral bending) in which they will operate in real-time; Implants, for example, should have sufficient structural integrity to withstand the forces operating in those

conditions[37]. Additionally, mechanical properties such as elastic modulus, tensile strength, ductility, fatigue life and strength, fretting fatigue life, wear properties of the implant are of significance[38].

Ideally, load-bearing implant materials such as orthopedic implant or dental implant should have mechanical properties (elastic modulus and strength) similar to that of the native bone to help avoid stress concentration or non-uniform stress distribution at the interface[39,40]. For example, in case of an orthopedic implant, the entire implant-bone region will experience "strain continuity" when subjected to load. Now if the implant's modulus is not effectively matched with that of bone, stress non-uniformity will arise between the implant and bone [for example, the stiffness of Ti, which is typically used in orthopedic implants, is higher than that of bone as shown in Fig 3(A)][40]. This effect is called "stress-shielding". If the stress difference is higher than the interfacial bonding strength, deboning may occur at the interface. Higher mismatch between the stiffness of the implant and that of native bones, may also cause bone resorption[41]. That is because the bone tissues remodel based on the prevailing stress conditions. Additionally, the stiffness of the interacting surface can regulate cell spreading and stem-cell phenotype changes[42].

To overcome these challenges, several biocompatible composites with mechanical properties similar to that of bone have been developed. Some reports on orthopedic implants have attempted to replicate the composite architecture of the natural bone itself. For instance, Liu *et al.* have replicated the hierarchically staggered architecture of collagen in bone by mineralizing tropo-collagen molecules in a hydroxyapatite (analogous to the bone mineral) precursor [Fig. 3-B2)][43]. The porous scaffold formed by freeze drying of the precursor [Fig. 3(B3-B4)] was found to regulate osteoblastic differentiation of stem cells and also exhibit suitable degradation rate (bio-resorption) to allow new bone ingrowth which accelerated bone regeneration [Fig. 3(B5-B6)]. Importantly, such porous implants have been shown to roughly match the mechanical properties of bone, enhance osteo-integration and promote vascularization through the implant thereby, providing pathways for bone in-growth through the pores, for stable long-term anchorage and biological fixation of the implant[44]. Porosity also enables easy passage of nutrients and ejection of cellular waste. However, porous materials often show accelerated wear or pore collapse at contact regions due to decreased contact area; this can result in particle release in addition to compromising the mechanical integrity of the scaffold[45,46]. Therefore, implants have to satisfy two opposing design criteria: increased porosity to improve

osteointegration, and sufficient mechanical strength to support physiologic loading. Additionally, for bone ingrowth, minimum porosity of the scaffold should be > 40% to enable cell infiltration and pore size should be within 50–800 μm for sufficient permeability[47,48]. The role of surface porosity in promoting angiogenesis has also been evaluated and a stronger angiogenic response is found when pore-sizes range between 30–40 μm[49].

A variety of porous scaffolds of different tissue type have also been fabricated by the electrospinning technique (listed in Table 2) that produces nanofibrous scaffolds for tissue engineering applications [Fig 3(C)]. The nanofibers present in the scaffolds could even be modulated into different dimensions (ranging from nano to micro-scale) and orientation (in either isotropic or anisotropic direction) to mimic the extra cellular matrix of different part of the body[50, 51]. The very high surface area to volume ratio and 3D interconnected porosity of the scaffolds enhance cell attachment and proliferation[52] [Fig. 3D]. Electrospun scaffolds incorporated with nanofillers (added to the polymer mixture before electrospinning) have also exhibited higher affinity for drugs and growth factors[53]. Additionally, biodegradable and naturally-derived polymers (*e.g.,* chitosan, silk) have been electrospun into randomly oriented or aligned fibrous scaffolds, thus providing additional means of tuning their degradation rates, mechanical properties and biological response for specific tissue applications[54,55,56,57,58]. On the other hand, biomaterials with well-defined porous framework have been developed by the 3-D printing technique. In fact, 3D printing also allows the biomaterials to be tailor-made to match the structural (anatomical) and mechanical properties of the implant region. For example, recently a 3-D mesh titanium scaffold for mandibular reconstruction were fabricated by 3-D printing involving electron beam melting (EBM) of Ti-6Al-4V medical-grade powder layer-by-layer[48]. A 3D reconstruction from CT scan provided the structural design (CAD) of the mandible (without soft tissue) which was then incorporated with 3-D mesh *via* finite element analysis to generate the internal microstructure of mandibular scaffold [Fig. 4(A1-A3)]. The design of the implant enables load distribution across the endplate and throughout the device. The open web/mesh architecture also maximizes bone incorporation while simultaneously conferring high-strength and lightweight properties.

Bioresorption is also an important biocompatibility feature desirable in biomaterials such as coronary stents. Stents are used to treat Coronary Artery Disease (where blood carrying vessels get clogged with arterial plaque resulting in obstructed blood flow) [Fig. 4(B1-B3)]. They have a regular network of struts to provide transient support to the affected vessels until healing has

completed (and also assist in deployment through a catheter-driven minimally-invasive procedure)[59]. However, the stent itself faces the risk of getting clogged due to plaque deposits over time (to overcome this problem drug-eluting stents have also been developed). Bioresorbable stents are another way this issue could be circumvented. Bioresorbable stents could self-degrade after the affected artery is healed. However, the bioresorption rate of the stent must match the natural healing rate of the artery. If not, then with successive resorption, the mechanical strength of the stent will progressively reduce. The stent could then pose the risk of premature collapse. To overcome these challenges, bioresorbable stents have been developed using poly(glycolic) acid, coated with an elastomer of poly(glycolide-co-caprolactone) [Figure 4(B1-B6)]. These composite stents fully resorb within 18 months in an ovine model, a duration long enough to ensure artery healing. Moreover, since these bioresorbable stents are polymer-based (in contrast to the traditional metal based stents), they could be used in cases of vessels (such as the superficial femoral artery) undergoing perpetual motion, that often results in kinking and fracturing of metal-based stents[60].

Biomechanical compatibility is of consideration in the organ printing technology too. That is because the mechanical properties of the printed structures is dependent on design parameters such as porosity that can be controlled by changing the printing parameters[61]. The surface roughness of the printed structure also plays a role in cell development and proliferation (discussed in detail in section III)[62]. Based on the type of the organ to be printed the cell type and the biomaterials are selected. For example: PCL/Chitosan are used for printing bone-scaffolds with higher porosity and higher modulus to facilitate osteogenic proliferation.[63] Similarly, collagen, gelatin and fibrin are used for printing organs like heart, brain, lungs. Most recently decellularized tissue-based hydrogels have also been synthesized (embedded with cardiomyocytes) and used for printing an entire human heart [Fig 4C][64]. Additionally, collagen (which is also one of the major compositional proteins of heart) has been used for printing human heart that exhibited rhythmic contractions and directional propagation of action potential [Fig. 4D]. These examples demonstrate the potential of combining 3D printing with the use of biocompatible naturally-derived constituents to pave way for printing of functional organs in the future[65,66].

Morphological compatibility: A placed implant or any biomedical device *in-vivo* must firmly engage with the neighboring hard or soft tissues[39]. A loose (or unstable) implant may become dysfunctional or operate less efficiently. It may also induce unintended and potentially harmful

tissue response (fibrosis) that could eventually cause the patient discomfort and pain. Close attachment of the implant with bone helps transmit stress from the implant to the bone without any appreciable relative motion between the two (minimize abrasion). In some cases, texturing the implant's surface may promote fixation by mechanical interlocking at the macro- or micro-scale with the neighboring tissues. In case of such textured/porous interfaces, the degree of bone ingrowth is found to be inversely proportional to the square root of the pore size[67]. A recent work investigates this strategy by applying silica nanoparticles (SiNPs) based coatings on titanium-based implants to generate a bioactive micro-rough surface that enhances osteo-integration as shown in Fig 5(A)[68]. The micro-rough surface was produced by layer-by-layer (LbL) assembly of SiNPs by using a recombinant of mussel adhesive protein that is biocompatible and improves adhesion of the coating to the implant surface. Basically, cell growth is promoted on rough surfaces because of improved cell attachment, possibly due to more anchoring sites. However, in the above case, cell growth was found to be highest when the roughness (S_a) ranged between 2.5 - 4.0 μm, beyond which, the cell counts were observed to drop. This demonstrates that while surface roughness facilitates bone integration, there is an upper limit to roughness beyond which the influence is insignificant. To understand that it must be acknowledged that cells are sensitive to micro-topography and can orient and migrate based on the underlying microstructural features[69-73]. So, a surface rendered with say, 25-μm particles creates a rough surface (roughness of the same order as the size of the cells and large biomolecules) recognizable by osteoblasts which promotes cell growth. On the other hand, assemblage of courser particles produces a roughness of relatively larger length-scales that osteoblast cells do not treat as rough anymore. Instead, the macro-rough surfaces act like a locally smooth surface[74]. On such smooth surfaces, cells attach and proliferate but they exhibit relatively low differentiation. On the other hand, on surfaces with micro-structural roughness (average roughness of 4-7 μm) cell differentiation is favored. Analysis of published clinical reports indicate that implant's surface roughness ranging from 1-10 μm is desirable for better implant integration with the adjacent native tissue[74]. Though in another study, sub-micron roughness on Ti implant surface also showed osteoblast differentiation[71]. Additionally, combination of nano-roughness, stiffness and conductivity is shown to enhance cell attachment for special cell types such as cardiomyocytes[Fig. 5B][75].

The role of biomaterial geometry in modulating foreign body response is also an important biocompatibility criterion. That is because the efficacy of an implanted biomaterial is often compromised by recognition of its presence by the body and subsequent foreign body

responses. Among the shapes tested, circular rods have been found to produce the least foreign body responses, followed by pentagonal and then triangular. Basically, biomaterials with smooth surfaces are likely to be more biocompatible than that with sharp edges[76]. A recent work suggests that spherical shaped implants have a significantly reduced fibrotic deposition (an indication of host immune response) regardless of the materials type (alginate hydrogels, polycaprolactone, polystyrene, glass, stainless steel)[77].

Some of the challenging areas in biomaterials research lie in remediation of compositionally- and mechanically-graded biological interfaces such as the bone-tendon interface that (compliant tendon to stiff bone) exhibit highly anisotropic mechanical property transition[78]. Development of grafts (such as those for repair of injured rotator cuff tissues, for example) need to have the capability to reduce stress concentrations at the interfaces between mineralized and un-mineralized tissues (*e.g.,* cartilage–bone, tendon–bone, ligament–bone interfaces) *via* mechanical-gradation[79,80]. For this purpose, differential stiffness biomaterials have been developed such as inverse opal scaffolds comprising graded hydroxyapatite (HAp) concentration [Fig. 5(C1)][81]. This is done by diffusion-limited transport of hydroxyapatite nanoparticles in a closely packed lattice of gelatin microbeads, which were later preferentially dissolved [Fig. 5(C2)]. The stiffness decreased with the graded reduction in HAp concentration, with the value changing from ≈ 2 GPa to 300 MPa (Where HAp concentration is least). The porous and graded mineral structure facilitated efficient transport of nutrients and metabolic wastes, and ensured homogenous cell distribution and high cell viability [Fig. 5(C3)][81].

Conclusion and Future Outlook

The biomaterials field has progressed from directly adopting industrial materials for biomedical application to developing advanced biomaterials with appropriately designed chemical and structural features. This has led to important advances being made in enhancing the biocompatibility of conventional (metal and alloy-based) biomaterials by incorporating porosity and textured/rough interfaces. Additionally, novel biomaterials mimicking the multi-scale (and mineralized or compositionally graded) designs of various biological tissues (bones, muscles, tendons, cardiac tissues *etc.*) have been developed. Such materials mimic the mechanical properties of the native tissues and alleviate stress concentration at the tissue-implant interface.

While many such biomaterials with unprecedented properties have been developed, complexity of these biomaterials remains a barrier for their translation into the clinic[82,83]. Furthermore, biocompatibility studies currently are focused more on materials rather than devices. This is a drawback since many medical devices are an aggregate of materials. Much of the preclinical testing is not conducted on the device but on the constituent materials only. Consequently, a biomaterial-design approach is gaining ground. A number of new technologies, such as combinatorial chemistry, next-generation sequencing (NGS), and high-content imaging are being integrated, to allow biomaterials engineers to take a holistic view of biomaterials development and investigate cell–material interactions along a range of biological conditions to ensure biocompatibility at the outset[84]. New modeling approaches such as molecular dynamics simulations and continuum models also allow for prediction of key parameters such as transport properties, degradation and failure modes, which are important indicators of biocompatibility as well[85]. On the other hand, 3D printing is enabling manufacturing of these biomaterials with different mechanical and structural properties in highly sophisticated ways[86].

Table 1A: Clinically used biomaterials made of metals and alloys

Materials	Applications
Stainless steel (type 316 &316L)	Bone plate and screws, intramedullary nails, surgical wire, metallic staples
CoCrMo alloy	Dentistry, artificial joint
CoNiCrMo alloy	Total knee and hip joint replacement (femoral stems), bone plate and screws, intramedullary nails, heart valve prosthesis (cage), surgical wire
Pure Ti	Bone implant porous coating, dental implants
Ti alloy (Ti6Al4V)	Total knee and hip joint replacement (tibial tray, femoral stem), intervertebral discs replacement, bone screw and plates, intramedullary nails, dental post, ligating pins
TiNi alloy (shape memory material)	Orthodontic dental archwire, vena cava filter, artificial heart (contractile artificial muscles), vascular stent, catheter guide wire, metallic staples
AgHg alloy	Dental amalgam
Gold & gold alloy	Dental restorative material (inlays, crowns and cusps)
Platinum group metals (Pt, Pd, Rh, Ir, Ru, and Os)	Pacemaker tip

Table 1B: Clinically used biomaterials made of ceramics

Materials	Applications
Non-resorbable or relatively bioinert	
Alumina (Al_2O_3)	Joint replacements, total hip joint replacement (femoral head & acetabular cup)
Zirconia (ZrO_2)	Total hip joint replacement (femoral head), bone implant, dental implant
Pyrolytic carbon (LTI Pyrolite®)	Heart valve prostheses occluders
Ultra-low-temperature isotropic (ULTI) carbon	Vascular graft coating
Biodegradable or resorbable	
Hydroxyapatite (HA)	Bone replacement material, bone plates and screws, bone implant coating, ocular implants, middle ear ossicle reconstruction
Aluminum–Calcium–Phosphate (ALCAP) Ceramics	Bone replacement material
Biocoral	Bone repair material
β-tricalcium phosphate	Bone cement, bone replacement material, bone augmentation, periodontal repair material
Bioactive or surface-reactive	
Bioglass and Ceravital™	Bone cement fillers, dental restorative material, metal implants coating

Table 1C: Clinically used biomaterials made of polymers

Materials	Applications
Polyvinylchloride (PVC)	Dialysis devices, ureter catheters
Polyethylene (PE)	Catheters, orthopedic implants

Ultra-high-molecular-weight polyethylene (UHMWPE)	Total hip joint replacement (acetabular cup), total knee joint replacement (tibial plateau and patellar surfaces), heart valve prostheses occluders
Polyurethane (PU)	Bone Implant coating, vascular grafts
Polyamide (nylon)	Nonabsorbable suture
Polypropylene (PP)	Monofilament sutures for intraocular lenses, finger joint prostheses, artificial ligaments, heart valve prosthesis stents, abdominal wall repair patch
Polytetrafluoroethylene (PTFE)	Catheter, vascular grafts, heart valve prostheses suture rings, stents, drain tubes
Polyethylenterephthalate (PET)	Vascular grafts, stents, heart valve prosthesis, nonabsorbable suture, abdominal wall repair patch
Polymethylmetacrylate (PMMA)	Contact lenses, implantable ocular lens, bone cement, dentures, maxillofacial prostheses
Silicone rubber (Silastic®)	Mammary implants, maxillofacial implants, heart valve prosthesis occluders
Polyoxymethylene (POM) (Delrin®)	Heart valve prosthesis
Polylactide （PLA）	Tissue suture anchor
Polyglycolide (Dexon® from American Cyanamid)	Wound closure, absorbable suture
Poly(glycolide-L-lactide) (Vicryl® from Ethicon)	Wound closure, absorbable suture, ligating pins, absorbable staples for skin and internal wound closures, hernia repair surgical mesh
Poly (glycolide-ε-caprolactone) (Monocryl® from Ethicon)	Wound closure
Poly (glycolide-trimethylene carbonate) (Maxon® from American Cyanamid)	Wound closure
Poly (ester-ether) (PDS® from Ethicon)	Wound closure, bone fracture fixation pins
Collagen	Soft tissue augmentation, corneal shield, hemostasis sponge in surgical applications, absorbable suture
Fibrin	Tissue adhesive

Table 1D: Clinically used biomaterials made of composites

Materials	Applications
Silicone rubber/SiO_2	Catheters
Silica/BIS-GMA Barium glass/BIS-GMA	Dental restorative material
Stainless steel/PEVA/PEMA (Cypher®)	Drug-eluting stent
CF/UHMWPE	Total knee joint replacement
PE/ tantalum	Total hip joint replacement
CoCr/PMMA	Bone cement in spinal stabilization surgery
PMMA/PHEMA	Contact lenses
CF/PEEK	Bone plates, total hip replacement
C/PTFE	Cochlear implants
Collagen-polysaccharide	Artificial skin

BIS-GMA: bis-phenol A glycidyl methacrylate, PEVA: poly (ethylene co-vinyl acetate), PEMA: poly (n- butyl methacrylate), CF: carbon fiber, C: carbon, PEEK: polyether-ether ketone

Table 2: Various electrospinning techniques used for development of different types of scaffolds for tissue engineering applications [87].

Strategy	Material	Pore Properties	Cell Infiltration
1. Conventional Electrospinning	Gelatin	Variation in fiber diameter from 110 nm to 600nm	Osteoblastic MG63 cell infiltration enhanced from 16 µm to 50 µm depth[88]
2. Sequential Electrospinning	PCL	Variation in fiber diameter from 200 nm to 1.5 µm in a gradient manner	NIH3T3 cells infiltration quickly through the microscale fibrous zone then slowed down through the nanoscale fibrous zone[89]
3. Concurrent Electrospinning	PLGA, PLGA-Collagen and PLGA-Collagen-Hydroxy apatite	Variation in fiber diameter and packing density from microscale to micro/nanoscale	MC3T3-E1 cell viability was increased by 2-fold from microscale scaffold to micro/nanoscale scaffold[90]
4. Electrospinning with sacrificial elements	Silk Fibroin and PEO	Variation in pore size 5.44 µm to 33.13 µm	Cells infiltration was enhanced up to 550 µm depth[91]
5. Electrospinning on rotating collectors	PLGA	Variation in pore size 21 µm to 132 µm	Cells infiltration was enhanced > 100 µm depth [92]
6. Electrospinning on patterned collectors	PCL	Variation in pore size by about 10 folds	Cells infiltration was enhanced up to 250 µm depth[93]
7. Cryogenic Electrospinning	PLA	Variation in pore volume from 900 μm^2 to 5000 μm^2	Cell infiltration was greater than 400 µm depth in vivo[94, 95]
8. Post-electrospinning Ultrasonication	Chitosan	Variation in porosity from 79% to 97%	Cell infiltration as enhanced by 1.4- fold[96]
9. Post-production electrospinning-gas foaming	PCL	Variation in porosity from 83.6% to 99.2%	Cells infiltration was seen only in gas foamed scaffold[97]
10. Post-production laser ablation	PLA	Variation in pore size from 21 to 130 µm	Enhanced cell migration and infiltration through ablated pores[98]

11. Emulsion electrospinning	PCL and Chitosan	Variation in pore size from 1 μm to 62 μm	Enhanced cell proliferation was seen within 3 weeks[99]
12. 3D printing co-electrospinning	PCL	Variation in fiber diameter and packing density	Enhanced cell proliferation was seen in3D/Espun scaffold than on 3D alone and Espun alone scaffolds[100]

Table 3: Surface Engineering to Improve Biocompatibility of Implants & Medical Devices

Biomaterials	Applications	Surface engineering	Notes	Reference
Collagen type I/ Ti6Al4V	Hard tissue implants	Activated Vapor Silanization functionalization	Method for protein immobilization	101
Pure Ti	Dental implants	Nonthermal atmospheric pressure plasma treatment	Enhanced hydrophilicity and protein adsorption	102
Ti-alloys		Thermal treatment	Improved bone healing	103
Ti-alloys		Ag NPs/nHA coating	Enhanced biocompatibility (cell adhesion, cell viability, cell morphology)	104
Ti-alloys		Air & oxygen atmosphere treatment	Air treated surface: TiO_2 formed Oxygen treated surface: TiO_2 & TiO	105
Ti-alloys		Electrochemical anodization (TiO_2 nano-network)	Improved hydrophilicity, bioactivity and biocompatibility	106
Zirconia		Blasted & acid etching	Comparable osteointegration to Ti implants	107
UHMWPE	Total joint replacement	Polyamide coating	Antibacterial, wound healing	108
CoCrMo alloy	Bone implants	TiN coating	Improved biocompatibility, anti-inflammation	109
Ti-alloys (Ti6Al4V)		HA coating	Curcumin and vitamin K2 delivery	110
Ti-alloys (Ti6Al4V)		PMMA/silica coating	Anticorrosive & bioactive coating	111
Ti-alloys		CaP anchorage	Improved early-stage osseointegration	112,113
Ti-alloys		Laser treatment	Ti-35Nb-7Zr-6Ta Antibacterial, improved osseointegration	114
Ti-alloys (TiNbSn)		Sulfuric acid anodic oxidation treatment	Improved biocompatibility & osseointegration	115
Ti-alloys (Ti6Al4V)		PCL/CaP/CNT coating	Improved cell adhesion	116
PEEK		Fast ambient-temperature sulfonation	Improved surface hydrophilicity	117
PLA	Cardiovascular stent	Heparin coating	Enhanced biocompatibility and anti-coagulation activity	118

nHA: nanosized hydroxyapatite, **CaP**: calcium phosphate, **CNT**: carbon nanotube, **PEEK**: polyether-ether ketone

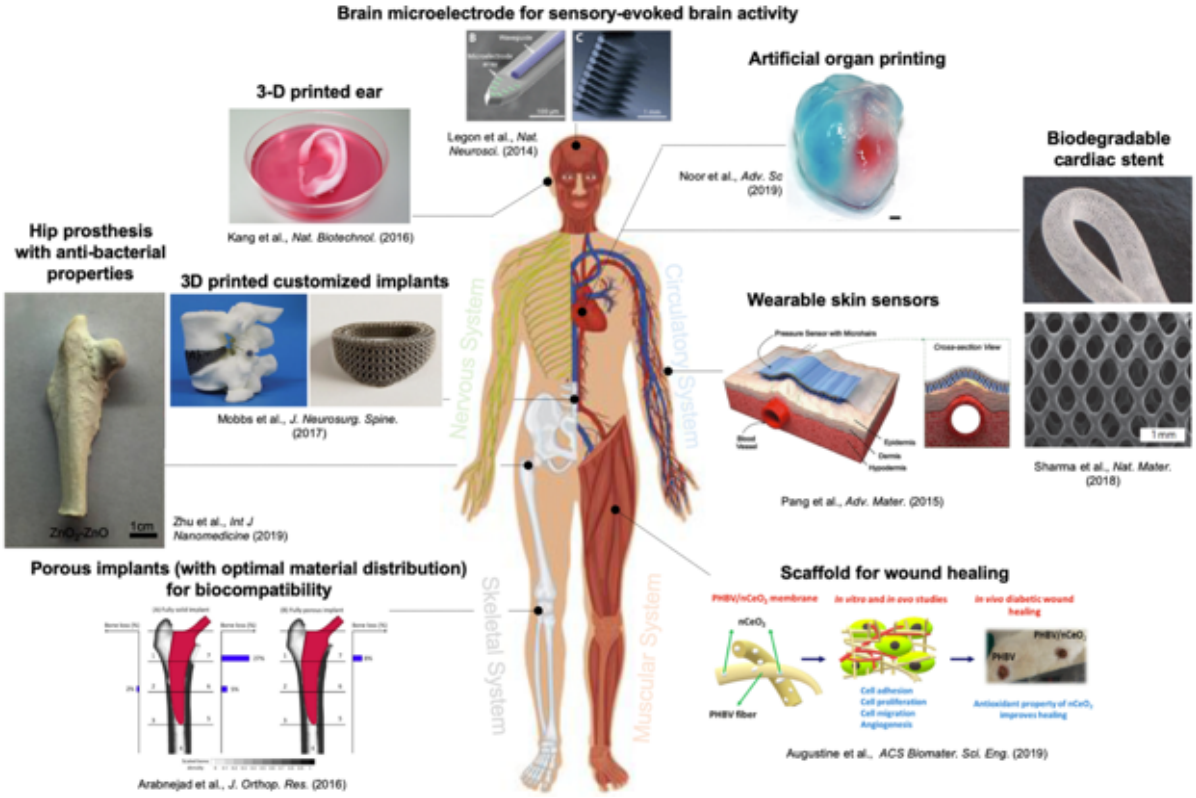

Figure 1: A schematic of recent biomaterials developed for application in a variety of tissue engineering applications.[119-127]

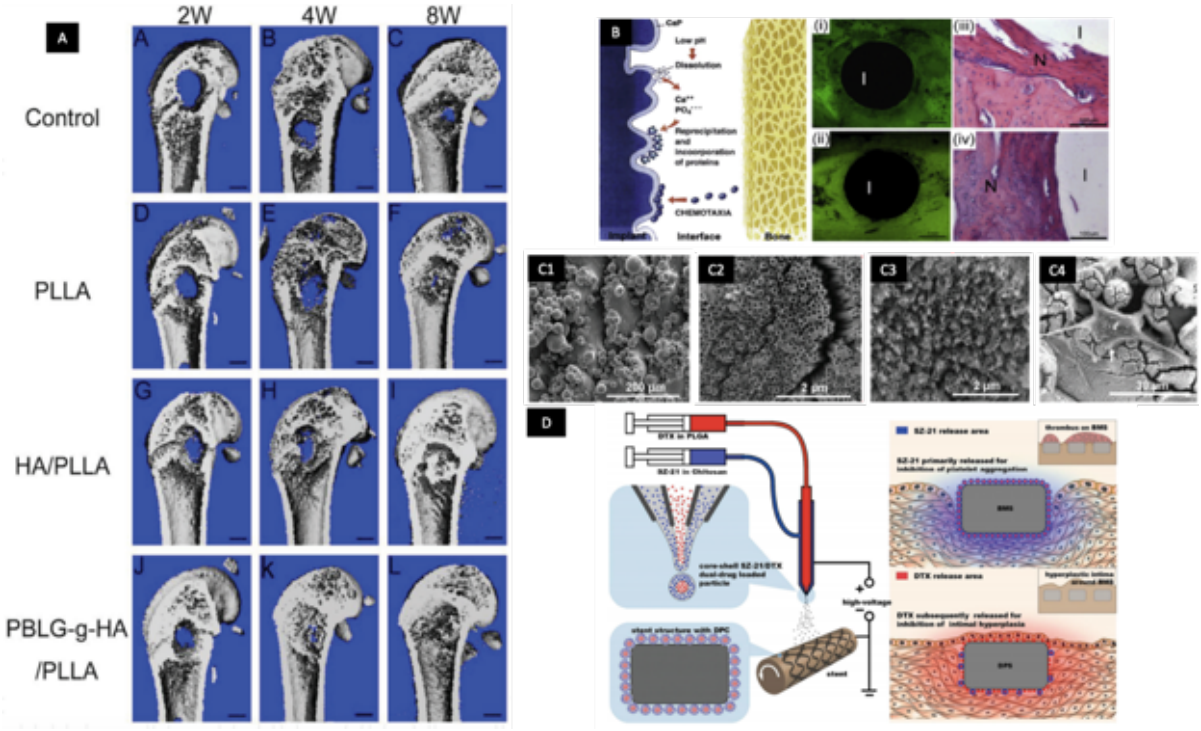

Figure 2: (A) Rapid bone regeneration in scaffold comprising hydroxyapatite (HA) as demonstrated in in-vivo studies of control and poly (L-lactic acid) (PLLA) vs. HA/PLLA and poly (γ-benzyl-L-glutamate)-modified hydroxyapatite/(poly (L-lactic acid) (PBLG-g-HA/PLLA) scaffolds at 2, 4, and 8 weeks after implantation.[30] (B) Schematic of enhanced osteointegration after Calcium Phosphate (Ca-P) coating of implants followed by the study showed the post-osteointegration H&E stained tissue sections of the implant coated with Ca-P and DCPC (Dicalcium phosphate dehydrate), respectively.[128] (C1) Surface of a 3D printed Ti alloy implant, covered with Ti nanotubes by anodization (C2)[32]. The same surface after HA coating (C3)[32]. Cells on the HA-coated porous surface exhibit a prominent stellate shape indicating better osteointegration (D) Stents coated with biomaterials (PLGA and chitosan) encapsulated with drugs and antibodies to promote endothelization and avoid platelet adhesion.[34]

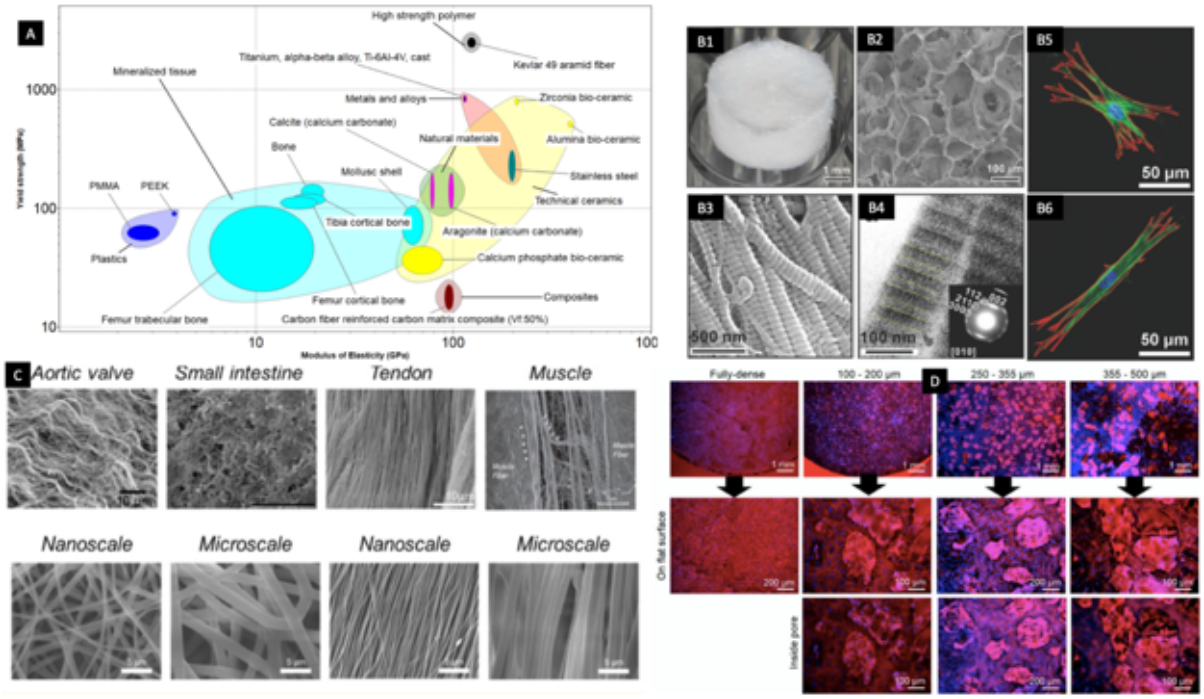

Figure 3: (A) Yield strength *vs.* elastic modulus of materials used in implants juxtaposed against bone (indicated as *B*). (B1 & B2) Photograph and microstructural view of a hierarchical scaffold comprising mineralized collagen with a typical cross-banding pattern of 66 ± 1.3 nm (B3)[43]. (B4) Nano-apatites minerals are seen as perpendicular repeating bands. The cells seeded on the hierarchical mineralized collagen scaffold exhibit a highly branched "osteocyte-like" shape (B5) in contrast to the control sample (B6)[43]. (C) Electrospinning of fibers forming mimics of ECM of distinct tissue type with controllable pore size (nanometers to micrometers). [50] (D) Implants with interconnected pores enhance cell attachment and proliferation[52]. Immunofluorescence images showing high cell proliferation inside the pores (captured after 10 days of cell inoculation). Red indicate actin cytoskeleton and blue indicate cell nuclei.

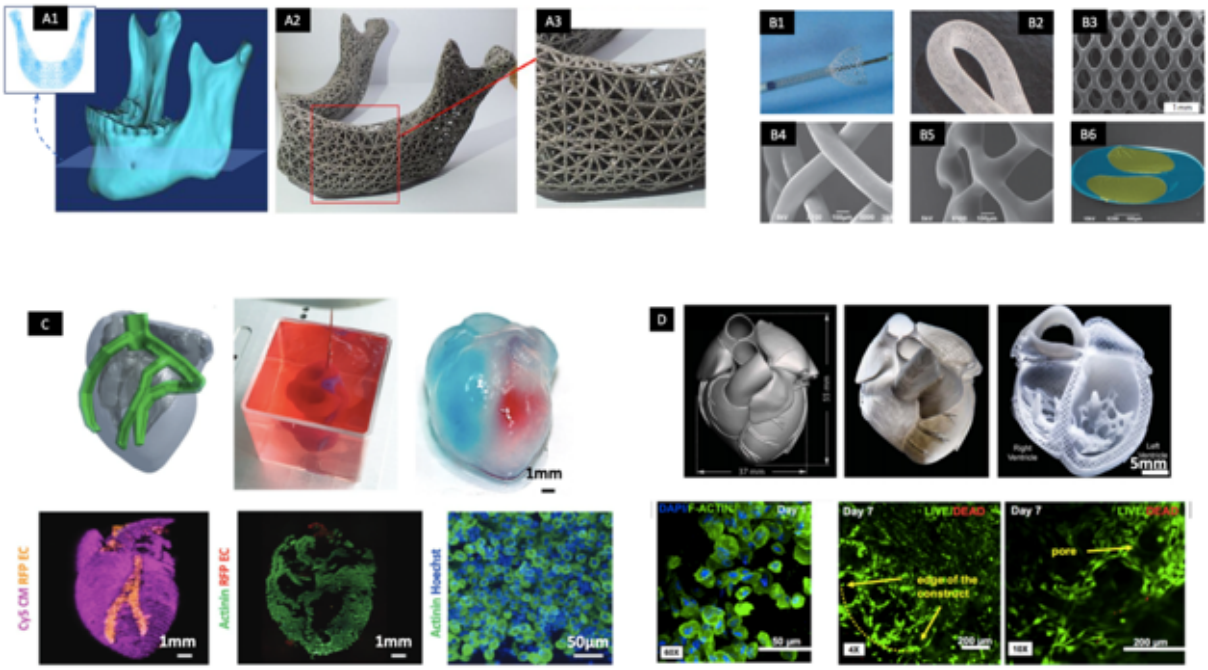

Figure 4: (A1) The 3D (design) scan of a human mandible and the finite element mesh (inset) generated from the design to manufacture a porous mandibular prosthesis[48]. (A2) The mandibular prosthesis is manufactured by a 3D printing technique (powder bed melting of Ti6Al4V powder by e-beam) (A3). (B1-B3) A strong, flexible, resorbable, self-expanding coronary stent[60]. (B4) The bioresorbable stent is made of PLGA base braid. (B5) The base braid (yellow region in cross-section shown in B6) is coated with an elastomer (blue region in B6) that provides a mechanism for the fibres to return to nominal diameter, imparting strength to the device. (C1) A 3D-printed human heart made from personalized bioink (decellularized tissue ink)[64]. CAD model of the heart is used as a template to print the organ inside a support bath. Printing of the vascularized tissue of heart is performed in a support bath. The left and the right ventricles are injected with dyes to indicate the hollow chambers, which are shown in red and blue, respectively. The 3D confocal images depicting the 3-D printed vascularized tissue structure of the heart (pink refers to cardiomyocytes and orange refers to that of the endothelial cells). The cardiomyocytes are characterized by immunostaining the sectioned heart where green label show the alpha sarcomeric actinin. 3-D printed human heart using naturally-derived collagen. (D) Viability and proliferation of cells (rBMSCs) in collagen (post-extrusion) for over 7 days of incubation (1st row)[65]. Collagen being a biocompatible material it is now used in its native form as a bioink to perform full organ bioprinting using a new technology called FRESH (freeform reversible embedding of suspended hydrogels).

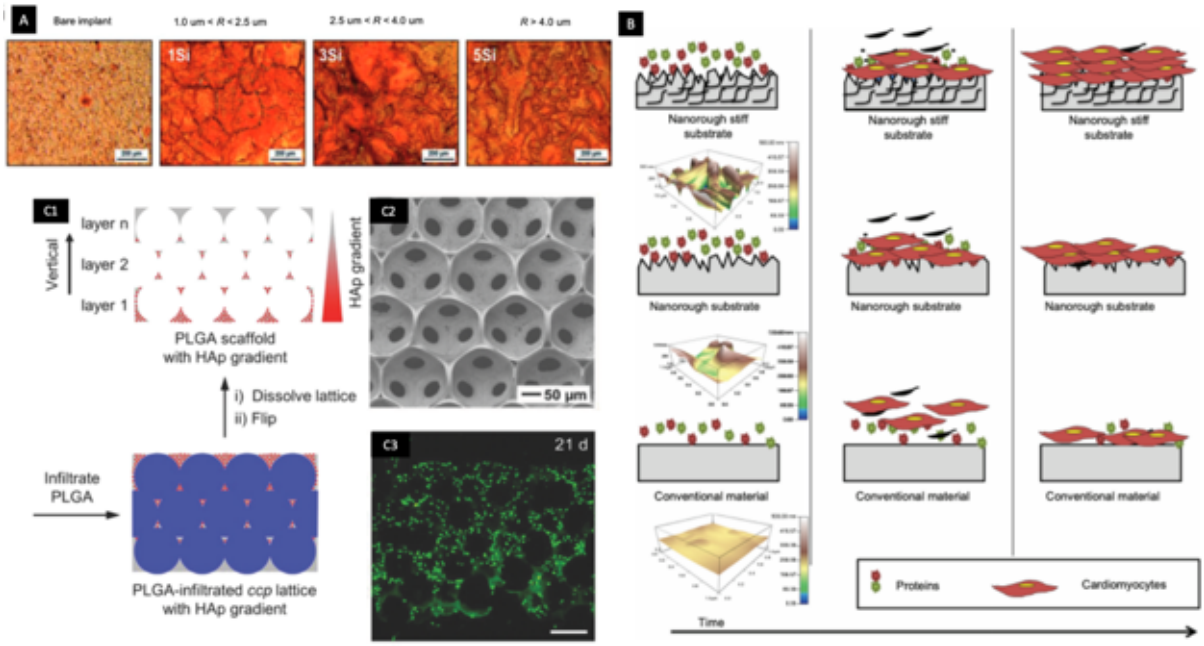

Figure 5: (A) Role of roughness in inducing cell differentiation. Microscopic images of stained (with Alizarin Red-S) pre-osteoblasts cells (at day 21) on the surface of micro-rough silica-nanoparticle-embedded coating on a Ti implant. (B) Role of nano-scale roughness, stiffness and surface conductivity in inducing cell attachment of cardiomoyocites. Row1: Bioactive surface made from PLGA:CNF mimics myocardium surface stiffness ensuring higher protein adsorption compared to conventional and plain nanorough surfaces. Row 2 and 3: Cartoon describing the concept in conventional materials and plain nanorough surface.[75] (C1) Illustration showing the generation of a gradient-stiffness scaffold having a mineral gradient (hydroxyapatite or HAp nanoparticles) in an inverse opal structure[81]. (C2) SEM image of the inverse opal scaffold. (C3) Live/dead staining of ASCs seeded in the scaffolds after 21 d of culture.

References

1 Tan, X., Tan, Y., Chow, C., Tor, S. & Yeong, W. Metallic powder-bed based 3D printing of cellular scaffolds for orthopaedic implants: A state-of-the-art review on manufacturing, topological design, mechanical properties and biocompatibility. *Materials Science and Engineering: C* **76**, 1328-1343 (2017).

2 Ducheyne, P. & Hastings, G. The Structure, Properties, and Functional Behavior of Biomaterials. *Metal and Ceramic Biomaterials: Volume II: Strength and Surface* (2018).

3 De Santis, R., Gloria, A. & Ambrosio, L. in *Biomedical Composites* 237-259 (Elsevier, 2017).

4 Hubbell, J. A. Biomaterials in tissue engineering. *Nature Biotechnology* **13**, 565 (1995).

5 Brovold, M. *et al.* in *Novel Biomaterials for Regenerative Medicine* 421-449 (Springer, 2018).

6 Faulk, D. M. & Badylak, S. F. in *Regenerative Medicine Applications in Organ Transplantation* 101-112 (Elsevier, 2014).

7 Williams, D. F. On the mechanisms of biocompatibility. *Biomaterials* **29**, 2941-2953 (2008).

8 Naahidi, S. *et al.* Biocompatibility of Engineered Nanoparticles for Drug Delivery. *Journal of Controlled Release* **166**, 182-194 (2013).

9 Bose, S. & Bandyopadhyay, A. in *Materials for Bone Disorders* 517-526 (Elsevier, 2017).

10 Arciola, C. R., Campoccia, D. & Montanaro, L. Implant infections: adhesion, biofilm formation and immune evasion. *Nature Reviews Microbiology* **16**, 397-409 (2018).

11 Ghasemi-Mobarakeh, L., Kolahreez, D., Ramakrishna, S. & Williams, D. Key terminology in biomaterials and biocompatibility. *Current Opinion in Biomedical Engineering* **10**, 45-50, doi:https://doi.org/10.1016/j.cobme.2019.02.004 (2019).

12 Hall-Stoodley, L., Costerton, J. W. & Stoodley, P. Bacterial biofilms: from the natural environment to infectious diseases. *Nature Reviews Microbiology* **2**, 95 (2004).

13 Costerton, J. W., Stewart, P. S. & Greenberg, E. P. Bacterial biofilms: a common cause of persistent infections. *Science* **284**, 1318-1322 (1999).

14 Revathi, A., Borrás, A. D., Muñoz, A. I., Richard, C. & Manivasagam, G. Degradation mechanisms and future challenges of titanium and its alloys for dental implant applications in oral environment. *Materials Science and Engineering: C* **76**, 1354-1368 (2017).

15 Anderson, J. M. Inflammatory response to implants. *ASAIO Transactions* **34**, 101-107 (1988).

16 Bose, S., Roy, M. & Bandyopadhyay, A. Recent Advances in Bone Tissue Engineering Scaffolds. *Trends in Biotechnology* **30**, 546-554 (2012).

17 Manam, N. *et al.* Study of corrosion in biocompatible metals for implants: A review. *Journal of Alloys and Compounds* **701**, 698-715 (2017).

18 Spriano, S., Yamaguchi, S., Baino, F. & Ferraris, S. A critical review of multifunctional titanium surfaces: New frontiers for improving osseointegration and host response, avoiding bacteria contamination. *Acta Biomaterialia* **79**, 1-22 (2018).

19 Mitchell, R. & Cotran, R. Acute and chronic inflammation in Robbins basic pathology. *Saunders*, 33-60 (2002).

20 Hanawa, T. Metal ion release from metal implants. *Materials Science and Engineering: C* **24**, 745-752 (2004).

21 Göpferich, A. Polymer degradation and erosion: mechanisms and applications. *European Journal of Pharmaceutics and Biopharmaceutics* **42**, 1-11 (1996).

22 Shi, L.-Y. *et al.* Tantalum-coated pedicle screws enhance implant integration. *Colloids and Surfaces B: Biointerfaces* **160**, 22-32 (2017).
23 Harun, W. *et al.* A comprehensive review of hydroxyapatite-based coatings adhesion on metallic biomaterials. *Ceramics International* **44**, 1250-1268 (2018).
24 Berman, A. T., Reid, J. S., Yanicko, J. D., Sih, G. C. & Zimmerman, M. Thermally induced bone necrosis in rabbits. Relation to implant failure in humans. *Clinical Orthopaedics and Related Research*, 284-292 (1984).
25 Cunningham, B. W., Hu, N., Zorn, C. M. & McAfee, P. C. Bioactive titanium calcium phosphate coating for disc arthroplasty: analysis of 58 vertebral end plates after 6-to 12-month implantation. *The Spine Journal* **9**, 836-845 (2009).
26 Kumari, R. & Majumdar, J. D. Studies on corrosion resistance and bio-activity of plasma spray deposited hydroxylapatite (HA) based TiO2 and ZrO2 dispersed composite coatings on titanium alloy (Ti-6Al-4V) and the same after post spray heat treatment. *Applied Surface Science* **420**, 935-943 (2017).
27 Zhao, X. *et al.* Fabrication of Al2O3 by anodic oxidation and hydrothermal synthesis of strong-bonding hydroxyapatite coatings on its surface. *Applied Surface Science* **470**, 959-969 (2019).
28 Grieco, P. W. *et al.* New alternate bearing surfaces in total hip arthroplasty: A review of the current literature. *Journal of Clinical Orthopaedics and Trauma* **9**, 7-16 (2018).
29 Albrektsson, T. Hydroxyapatite-coated implants: a case against their use. *Journal of Oral and Maxillofacial Surgery* **56**, 1312-1326 (1998).
30 Liao, L. *et al.* Osteogenic properties of PBLG-g-HA/PLLA nanocomposites. *PloS One* **9**, e105876 (2014).
31 Hu, J. *et al.* Porous nanofibrous PLLA scaffolds for vascular tissue engineering. *Biomaterials* **31**, 7971-7977 (2010).
32 Qin, J. *et al.* Micro-and nano-structured 3D printed titanium implants with a hydroxyapatite coating for improved osseointegration. *Journal of Materials Chemistry B* **6**, 3136-3144 (2018).
33 Schmidt, T. & Abbott, J. Coronary stents: history, design, and construction. *Journal of Clinical Medicine* **7**, 126 (2018).
34 Du, R. *et al.* Design and testing of hydrophobic core/hydrophilic shell nano/micro particles for drug-eluting stent coating. *NPG Asia Materials* **10**, 642 (2018).
35 Ichihashi, S. *et al.* Bio-Based Covered Stents: The Potential of Biologically Derived Membranes. *Tissue Engineering Part B: Reviews* **25**, 135-151 (2019).
36 Lenz-Habijan, T. *et al.* Hydrophilic stent coating inhibits platelet adhesion on stent surfaces: initial results in vitro. *Cardiovascular and Interventional Radiology* **41**, 1779-1785 (2018).
37 Dvir, T., Timko, B. P., Kohane, D. S. & Langer, R. Nanotechnological strategies for engineering complex tissues. *Nature Nanotechnology* **6**, 13 (2011).
38 Wang, C. J. & Hazlehurst, K. B. Orthopedic Implant Design and Analysis: Potential of 3D/4D Bioprinting. *3D and 4D Printing in Biomedical Applications: Process Engineering and Additive Manufacturing*, 423-442 (2019).
39 Oshida, Y. *Surface Engineering and Technology for Biomedical Implants*. (Momentum Press, 2014).
40 Navarro, M., Michiardi, A., Castano, O. & Planell, J. Biomaterials in orthopaedics. *Journal of the Royal Society Interface* **5**, 1137-1158 (2008).
41 Arabnejad Khanoki, S. & Pasini, D. Multiscale design and multiobjective optimization of orthopedic hip implants with functionally graded cellular material. *Journal of Biomechanical Engineering* **134** (2012).

42 Wen, J. H. *et al.* Interplay of matrix stiffness and protein tethering in stem cell differentiation. *Nature Materials* **13**, 979 (2014).

43 Liu, Y. *et al.* Hierarchically staggered nanostructure of mineralized collagen as a bone-grafting scaffold. *Advanced Materials* **28**, 8740-8748 (2016).

44 Fu, Q., Jia, W., Lau, G. Y. & Tomsia, A. P. Strength, toughness, and reliability of a porous glass/biopolymer composite scaffold. *Journal of Biomedical Materials Research Part B: Applied Biomaterials* **106**, 1209-1217 (2018).

45 Vardavoulias, M., Jouanny-Tresy, C. & Jeandin, M. Sliding-wear behaviour of ceramic particle-reinforced high-speed steel obtained by powder metallurgy. *Wear* **165**, 141-149 (1993).

46 Bragdon, C. R., Jasty, M., Greene, M., Rubash, H. E. & Harris, W. H. Biologic fixation of total hip implants: Insights gained from a series of canine studies. *JBJS* **86**, 105-117 (2004).

47 Harrysson, O. L., Cansizoglu, O., Marcellin-Little, D. J., Cormier, D. R. & West II, H. A. Direct metal fabrication of titanium implants with tailored materials and mechanical properties using electron beam melting technology. *Materials Science and Engineering: C* **28**, 366-373 (2008).

48 Yan, R. *et al.* Electron beam melting in the fabrication of three-dimensional mesh titanium mandibular prosthesis scaffold. *Scientific Reports* **8**, 750 (2018).

49 Madden, L. R. *et al.* Proangiogenic scaffolds as functional templates for cardiac tissue engineering. *Proceedings of the National Academy of Sciences* **107**, 15211-15216 (2010).

50 Jun, I., Han, H.-S., Edwards, J. & Jeon, H. Electrospun fibrous scaffolds for tissue engineering: Viewpoints on architecture and fabrication. *International Journal of Molecular Sciences* **19**, 745 (2018).

51 Bertuoli, P. T. *et al.* Electrospun Conducting and Biocompatible Uniaxial and Core–Shell Fibers Having Poly (lactic acid), Poly (ethylene glycol), and Polyaniline for Cardiac Tissue Engineering. *ACS Omega* **4**, 3660-3672 (2019).

52 Civantos, A. *et al.* Balancing Porosity and Mechanical Properties of Titanium Samples to Favor Cellular Growth against Bacteria. *Metals* **9**, 1039 (2019).

53 Mochane, M. J., Motsoeneng, T. S., Sadiku, E. R., Mokhena, T. C. & Sefadi, J. S. Morphology and Properties of Electrospun PCL and Its Composites for Medical Applications: A Mini Review. *Applied Sciences* **9**, 2205 (2019).

54 Luo, B. *et al.* Electrospun nanofibers facilitate better alignment, differentiation, and long-term culture in an in vitro model of the neuromuscular junction (NMJ). *Biomaterials Science* **6**, 3262-3272 (2018).

55 Zarrintaj, P., Saeb, M. R., Ramakrishna, S. & Mozafari, M. Biomaterials selection for neuroprosthetics. *Current Opinion in Biomedical Engineering* **6**, 99-109 (2018).

56 Kouhi, M., Fathi, M., Prabhakaran, M. P., Shamanian, M. & Ramakrishna, S. Enhanced proliferation and mineralization of human fetal osteoblast cells on PHBV-bredigite nanofibrous scaffolds. *Materials Today: Proceedings* **5**, 15702-15709 (2018).

57 Kouhi, M., Fathi, M., Prabhakaran, M. P., Shamanian, M. & Ramakrishna, S. Poly L lysine-modified PHBV based nanofibrous scaffolds for bone cell mineralization and osteogenic differentiation. *Applied Surface Science* **457**, 616-625 (2018).

58 Rad, M. M. *et al.* Fabrication and characterization of two-layered nanofibrous membrane for guided bone and tissue regeneration application. *Materials Science and Engineering: C* **80**, 75-87 (2017).

59 McCormick, C. in *Functionalised Cardiovascular Stents* 3-26 (Elsevier, 2018).

60 Sharma, U. *et al.* The development of bioresorbable composite polymeric implants with high mechanical strength. *Nature materials* **17**, 96 (2018).

61 Gao, G., Huang, Y., Schilling, A. F., Hubbell, K. & Cui, X. Organ bioprinting: are we there yet? *Advanced Healthcare Materials* **7**, 1701018 (2018).
62 Dong, L., Wang, S.-J., Zhao, X.-R., Zhu, Y.-F. & Yu, J.-K. 3D-printed poly (ε-caprolactone) scaffold integrated with cell-laden chitosan hydrogels for bone tissue engineering. *Scientific Reports* **7**, 13412 (2017).
63 Georgopoulou, A., Kaliva, M., Vamvakaki, M. & Chatzinikolaidou, M. Osteogenic potential of pre-osteoblastic cells on a chitosan-graft-polycaprolactone copolymer. *Materials* **11**, 490 (2018).
64 Noor, N. *et al.* 3D Printing of Personalized Thick and Perfusable Cardiac Patches and Hearts. *Advanced Science*, 1900344 (2019).
65 Lee, A. *et al.* 3D bioprinting of collagen to rebuild components of the human heart. *Science* **365**, 482-487 (2019).
66 Moncal, K. K., Ozbolat, V., Datta, P., Heo, D. N. & Ozbolat, I. T. Thermally-controlled extrusion-based bioprinting of collagen. *Journal of Materials Science: Materials in Medicine* **30**, 55 (2019).
67 Clemow, A., Weinstein, A., Klawitter, J., Koeneman, J. & Anderson, J. Interface mechanics of porous titanium implants. *Journal of Biomedical Materials Research* **15**, 73-82 (1981).
68 Jo, Y. K., Choi, B. H., Kim, C. S. & Cha, H. J. Diatom-inspired silica nanostructure coatings with controllable microroughness using an engineered mussel protein glue to accelerate bone growth on titanium-based implants. *Advanced Materials* **29**, 1704906 (2017).
69 Trappmann, B. *et al.* Extracellular-matrix tethering regulates stem-cell fate. *Nature Materials* **11**, 642 (2012).
70 Stevens, M. M. & George, J. H. Exploring and engineering the cell surface interface. *Science* **310**, 1135-1138 (2005).
71 Zinger, O. *et al.* Differential regulation of osteoblasts by substrate microstructural features. *Biomaterials* **26**, 1837-1847 (2005).
72 Engler, A. J., Sen, S., Sweeney, H. L. & Discher, D. E. Matrix elasticity directs stem cell lineage specification. *Cell* **126**, 677-689 (2006).
73 Dalby, M. J., Gadegaard, N. & Oreffo, R. O. Harnessing nanotopography and integrin–matrix interactions to influence stem cell fate. *Nature materials* **13**, 558-569 (2014).
74 Ellingsen, J. E. Surface configurations of dental implants. *Periodontology 2000* **17**, 36-46 (1998).
75 Stout, D. A., Yoo, J., Santiago-Miranda, A. N. & Webster, T. J. Mechanisms of greater cardiomyocyte functions on conductive nanoengineered composites for cardiovascular application. *International journal of nanomedicine* **7**, 5653 (2012).
76 Matlaga, B. F., Yasenchak, L. P. & Salthouse, T. N. Tissue response to implanted polymers: the significance of sample shape. *Journal of Biomedical Materials Research* **10**, 391-397 (1976).
77 Veiseh, O. *et al.* Size-and shape-dependent foreign body immune response to materials implanted in rodents and non-human primates. *Nature Materials* **14**, 643 (2015).
78 Rossetti, L. *et al.* The microstructure and micromechanics of the tendon–bone insertion. *Nature Materials* **16**, 664 (2017).
79 Patel, S. *et al.* Integrating soft and hard tissues via interface tissue engineering. *Journal of Orthopaedic Research®* **36**, 1069-1077 (2018).
80 Kokkinis, D., Bouville, F. & Studart, A. R. 3D printing of materials with tunable failure via bioinspired mechanical gradients. *Advanced Materials* **30**, 1705808 (2018).

81 Zhu, C., Qiu, J., Pongkitwitoon, S., Thomopoulos, S. & Xia, Y. Inverse Opal Scaffolds with Gradations in Mineral Content for Spatial Control of Osteogenesis. *Advanced Materials* **30**, 1706706 (2018).
82 Darnell, M. & Mooney, D. J. Leveraging advances in biology to design biomaterials. *Nature Materials* **16**, 1178-1185 (2017).
83 Prestwich, G. D. *et al.* What is the greatest regulatory challenge in the translation of biomaterials to the clinic? *Science Translational Medicine* **4**, 160cm114-160cm114 (2012).
84 Vegas, A. J. *et al.* Combinatorial hydrogel library enables identification of materials that mitigate the foreign body response in primates. *Nature Biotechnology* **34**, 345 (2016).
85 Redondo, A. & LeSar, R. Modeling and simulation of biomaterials. *Annu. Rev. Mater. Res.* **34**, 279-314 (2004).
86 Kolesky, D. B., Homan, K. A., Skylar-Scott, M. A. & Lewis, J. A. Three-dimensional bioprinting of thick vascularized tissues. *Proceedings of the National Academy of Sciences* **113**, 3179-3184 (2016).
87 Ameer, J. M., PR, A. K. & Kasoju, N. Strategies to tune electrospun scaffold porosity for effective cell response in tissue engineering. *Journal of Functional Biomaterials* **10**, 30 (2019).
88 Sisson, K., Zhang, C., Farach-Carson, M. C., Chase, D. B. & Rabolt, J. F. Fiber diameters control osteoblastic cell migration and differentiation in electrospun gelatin. *Journal of Biomedical Materials Research Part A* **94**, 1312-1320 (2010).
89 Kim, J.-s., Im, B. G., Jin, G. & Jang, J.-H. Tubing-electrospinning: a one-step process for fabricating fibrous matrices with spatial, chemical, and mechanical gradients. *ACS Applied Materials & Interfaces* **8**, 22721-22731 (2016).
90 Kwak, S., Haider, A., Gupta, K. C., Kim, S. & Kang, I.-K. Micro/nano multilayered scaffolds of PLGA and collagen by alternately electrospinning for bone tissue engineering. *Nanoscale Research Letters* **11**, 323 (2016).
91 Wang, K. *et al.* Creation of macropores in electrospun silk fibroin scaffolds using sacrificial PEO-microparticles to enhance cellular infiltration. *Journal of Biomedical Materials Research Part A: An Official Journal of The Society for Biomaterials, The Japanese Society for Biomaterials, and The Australian Society for Biomaterials and the Korean Society for Biomaterials* **101**, 3474-3481 (2013).
92 Zhu, X., Cui, W., Li, X. & Jin, Y. Electrospun fibrous mats with high porosity as potential scaffolds for skin tissue engineering. *Biomacromolecules* **9**, 1795-1801 (2008).
93 Vaquette, C. & Cooper-White, J. J. Increasing electrospun scaffold pore size with tailored collectors for improved cell penetration. *Acta Biomaterialia* **7**, 2544-2557 (2011).
94 Leong, M. F., Rasheed, M. Z., Lim, T. C. & Chian, K. S. In vitro cell infiltration and in vivo cell infiltration and vascularization in a fibrous, highly porous poly (d, l-lactide) scaffold fabricated by cryogenic electrospinning technique. *Journal of Biomedical Materials Research Part A: An Official Journal of The Society for Biomaterials, The Japanese Society for Biomaterials, and The Australian Society for Biomaterials and the Korean Society for Biomaterials* **91**, 231-240 (2009).
95 Leong, M. F., Chan, W. Y. & Chian, K. S. Cryogenic electrospinning: proposed mechanism, process parameters and its use in engineering of bilayered tissue structures. *Nanomedicine* **8**, 555-566 (2013).
96 Gu, B. K. *et al.* Fabrication of sonicated chitosan nanofiber mat with enlarged porosity for use as hemostatic materials. *Carbohydrate Polymers* **97**, 65-73 (2013).

97 Jiang, J. *et al.* Expanding two-dimensional electrospun nanofiber membranes in the third dimension by a modified gas-foaming technique. *ACS Biomaterials Science & Engineering* **1**, 991-1001 (2015).
98 Lee, B. L.-P. *et al.* Femtosecond laser ablation enhances cell infiltration into three-dimensional electrospun scaffolds. *Acta Biomaterialia* **8**, 2648-2658 (2012).
99 Pal, P. *et al.* Nano-/microfibrous cotton-wool-like 3D scaffold with core–shell architecture by emulsion electrospinning for skin tissue regeneration. *ACS Biomaterials Science & Engineering* **3**, 3563-3575 (2017).
100 Mellor, L. F. *et al.* Fabrication and evaluation of electrospun, 3D-bioplotted, and combination of electrospun/3D-bioplotted scaffolds for tissue engineering applications. *BioMed Research International* **2017** (2017).
101 Rezvanian, P. *et al.* Enhanced Biological Response of AVS-Functionalized Ti-6Al-4V Alloy through Covalent Immobilization of Collagen. *Scientific Reports* **8**, 1-11, doi:10.1038/s41598-018-21685-3 (2018).
102 Jeong, W. S., Kwon, J. S., Choi, E. H. & Kim, K. M. The Effects of Non-Thermal Atmospheric Pressure Plasma treated Titanium Surface on Behaviors of Oral Soft Tissue Cells. *Scientific Reports* **8**, 1-13, doi:10.1038/s41598-018-34402-x (2018).
103 Scarano, A., Crocetta, E., Quaranta, A. & Lorusso, F. Influence of the thermal treatment to address a better osseointegration of Ti6Al4V Dental Implants: Histological and histomorphometrical study in a rabbit model. *BioMed Research International* **2018**, 2349698-2349698, doi:10.1155/2018/2349698 (2018).
104 Salaie, R. N., Besinis, A., Le, H., Tredwin, C. & Handy, R. D. The biocompatibility of silver and nanohydroxyapatite coatings on titanium dental implants with human primary osteoblast cells. *Materials Science and Engineering C* **107**, 110210-110210, doi:10.1016/j.msec.2019.110210 (2020).
105 Khodaei, M., Alizadeh, A. & Hosseini, H. R. M. Effect of Oxidizing Atmosphere on the Surface of Titanium Dental Implant Material. *Journal of Bionic Engineering* **16**, 1052-1060, doi:10.1007/s42235-019-0117-1 (2019).
106 Yang, W.-E. & Huang, H.-H. Multiform TiO2 nano-network enhances biological response to titanium surface for dental implant applications. *Applied Surface Science* **471**, 1041-1052 (2019).
107 Kubasiewicz-Ross, P., Hadzik, J. & Dominiak, M. Osseointegration of zirconia implants with 3 varying surface textures and a titanium implant: A histological and micro-CT study. *Advances in Clinical and Experimental Medicine* **27**, 1173-1179, doi:10.17219/acem/69246 (2018).
108 Hassanein, N., Bougherara, H. & Amleh, A. In- vitro evaluation of the bioactivity and the biocompatibility of a novel coated UHMWPE biomaterial for biomedical applications. *Journal of the Mechanical Behavior of Biomedical Materials* **101**, 103409-103409, doi:10.1016/j.jmbbm.2019.103409 (2020).
109 Lohberger, B. *et al.* CoCrMo surface modifications affect biocompatibility, adhesion, and inflammation in human osteoblasts. *Scientific Reports* **10**, 1682-1682, doi:10.1038/s41598-020-58742-9 (2020).
110 Sarkar, N. & Bose, S. Controlled delivery of curcumin and vitamin K2 from HA-coated Ti implant for enhanced in vitro chemoprevention, osteogenesis and in vivo osseointegration. *ACS Applied Materials & Interfaces* **10**, doi:10.1021/acsami.9b22474 (2020).
111 Harb, S. V. *et al.* PMMA-silica nanocomposite coating: Effective corrosion protection and biocompatibility for a Ti6Al4V alloy. *Materials Science and Engineering: C* **110**, 110713-110713, doi:10.1016/j.msec.2020.110713 (2020).

112 Chen, J. C. *et al.* In vivo studies of titanium implant surface treatment by sandblasted, acid-etched and further anchored with ceramic of tetracalcium phosphate on osseointegration. *Journal of the Australian Ceramic Society* **55**, 799-806, doi:10.1007/s41779-018-00292-5 (2019).
113 Bose, S., Banerjee, D., Shivaram, A., Tarafder, S. & Bandyopadhyay, A. Calcium phosphate coated 3D printed porous titanium with nanoscale surface modification for orthopedic and dental applications. *Materials and Design* **151**, 102-112, doi:10.1016/j.matdes.2018.04.049 (2018).
114 Donaghy, C. L. *et al.* Fibre laser treatment of beta TNZT titanium alloys for load-bearing implant applications: Effects of surface physical and chemical features on mesenchymal stem cell response and Staphylococcus aureus bacterial attachment. *Coatings* **9**, 186-186, doi:10.3390/COATINGS9030186 (2019).
115 Kunii, T. *et al.* Improved osseointegration of a TiNbSn alloy with a low Young's modulus treated with anodic oxidation. *Scientific Reports* **9**, 1-10, doi:10.1038/s41598-019-50581-7 (2019).
116 Montañez, N. D. *et al.* Functional evaluation and testing of a newly developed Teleost's Fish Otolith derived biocomposite coating for healthcare. *Scientific reports* **10**, 258-258, doi:10.1038/s41598-019-57128-w (2020).
117 Wang, W., Luo, C. J., Huang, J. & Edirisinghe, M. PEEK surface modification by fast ambient-temperature sulfonation for bone implant applications. *Journal of the Royal Society Interface* **16**, doi:10.1098/rsif.2018.0955 (2019).
118 Lee, S. J. *et al.* Heparin coating on 3D printed poly (l-lactic acid) biodegradable cardiovascular stent via mild surface modification approach for coronary artery implantation. *Chemical Engineering Journal* **378**, 122116-122116, doi:10.1016/j.cej.2019.122116 (2019).
119 Legon, W. *et al.* Transcranial focused ultrasound modulates the activity of primary somatosensory cortex in humans. *Nature Neuroscience* **17**, 322-329, doi:10.1038/nn.3620 (2014).
120 Kang, H.-W. *et al.* A 3D bioprinting system to produce human-scale tissue constructs with structural integrity. *Nature Biotechnology* **34**, 312-319, doi:10.1038/nbt.3413 (2016).
121 Ralph, J. M., Marc, C., Robert, T., Chester, E. S. & Kevin, P. The utility of 3D printing for surgical planning and patient-specific implant design for complex spinal pathologies: case report. *Journal of Neurosurgery: Spine SPI* **26**, 513-518, doi:10.3171/2016.9.SPINE16371 (2017).
122 Zhu, Y. *et al.* 3D printed zirconia ceramic hip joint with precise structure and broad-spectrum antibacterial properties. *International Journal of Nanomedicine* **14**, 5977-5987, doi:10.2147/IJN.S202457 (2019).
123 Arabnejad, S., Johnston, B., Tanzer, M. & Pasini, D. Fully porous 3D printed titanium femoral stem to reduce stress-shielding following total hip arthroplasty. *Journal of Orthopaedic Research* **35**, 1774-1783, doi:10.1002/jor.23445 (2017).
124 Augustine, R. *et al.* Cerium Oxide Nanoparticle Incorporated Electrospun Poly(3-hydroxybutyrate-co-3-hydroxyvalerate) Membranes for Diabetic Wound Healing Applications. *ACS Biomaterials Science & Engineering* **6**, 58-70, doi:10.1021/acsbiomaterials.8b01352 (2020).
125 Pang, C. *et al.* Highly Skin-Conformal Microhairy Sensor for Pulse Signal Amplification. *Advanced Materials* **27**, 634-640, doi:10.1002/adma.201403807 (2015).
126 Sharma, U. *et al.* The development of bioresorbable composite polymeric implants with high mechanical strength. *Nature Materials* **17**, 96-103, doi:10.1038/nmat5016 (2018).

127 Noor, N. *et al.* 3D Printing of Personalized Thick and Perfusable Cardiac Patches and Hearts. *Advanced Science* **6**, 1900344, doi:10.1002/advs.201900344 (2019).
128 Su, Y. *et al.* Biofunctionalization of metallic implants by calcium phosphate coatings. *Bioactive Materials* **4**, 196-206 (2019).